Desalination and Water Treatment
www.deswater.com
doi: 10.1080/19443994.2015.1013992

57 (2016) 7196–7208
April

Taylor & Francis
Taylor & Francis Group

S. cerevisiae cells modified with nZVI: a novel magnetic biosorbent for nickel removal from aqueous solutions

Ulker Asli Guler[a], Mehtap Ersan[b,*]

[a]*Engineering Faculty, Department of Environmental Engineering, Cumhuriyet University, Sivas 58140, Turkey, email: ulkerasli@gmail.com*
[b]*Engineering Faculty, Department of Chemical Engineering, Cumhuriyet University, Sivas 58140, Turkey, Tel. +90 0346 219 10/2243; Fax: +90 346 219 11 77; email: gorgun7@hotmail.com*

Received 26 June 2014; Accepted 27 January 2015

ABSTRACT

The present study was conducted to evaluate the applicability of *S. cerevisiae* cells modified with nZVI (magnetic biosorbent) for the Ni(II) ions removal from aqueous solutions. This composite was synthesized in ethanol using a borohydride reduction method in atmospheric conditions and characterized by FTIR, XRD, and SEM analyses. Batch experiments were examined the effects of initial solution pH, magnetic biosorbent amount, contact time, initial Ni(II) concentration, and temperature. Langmuir, Freundlich, Dubinin–Radushkevich, and Temkin isotherm models were applied to the equilibrium data. The maximum biosorption capacity of the magnetic biosorbent was found to be relatively high (54.23 mg/g). The reductive power of the Fe^0 and functional groups on the yeast cell surface contributed to the removal of Ni(II) ions. The kinetics data were best described by the pseudo-second-order kinetics model. Thermodynamics parameters were calculated from the experimental data. Ni(II) removal onto magnetic biosorbent was favorable, physicochemical in nature. Also, the Ni(II) removal onto magnetic biosorbent decreased with increasing in Na concentration in aqueous solutions. The results of this study suggest that the magnetic biosorbent is effective for Ni(II) removal from aqueous solutions.

Keywords: Ni(II) removal; *S. cerevisiae*; *S. cerevisiae*-nZVI composite; Reduction; Biosorption

1. Introduction

Ni(II) is one of the most common pollutants in wastewaters related to mining and metallurgy, stainless steel, aircraft industries, nickel electroplating, battery and manufacturing, pigments and ceramic industries, domestic contaminants, and waste materials. Wastewaters from paint-ink production and porcelain enameling industries contain Ni(II) concentrations ranging from 0–40 to 0.25–67 mg/L, respectively. In plating plants, Ni(II) concentrations can approach 2–205 and 2–900 mg/L (rinse waters). In mine drainage, Ni(II) concentrations can approach 0.19–0.51, 0.46–3.4 (acidic), and 0.01–0.18 mg/L (alkaline) [1,2]. Ni(II) ion intake above permissible levels can cause harmful health effects such as pulmonary fibrosis, renal oedema, skin dermatitis, and gastrointestinal distress (e.g. nausea, vomiting, and diarrhea) [3]. Hence, the removal of Ni(II) from the wastewater is of significant impor-tance [4,5]. Some conventional methods such as coagulation–flocculation, chemical precipitation, ozonation, membrane filtration,

*Corresponding author.

sedimentation, ion exchange, and adsorption have been used for treating water contaminated with Ni(II) ions [4,6,7]. Of these methods, adsorption is a highly efficient and economical technique [8].

Iron nanoparticles (nZVI) in powder or granular form have been applied as a reactive material in permeable reactive barriers to remove different contaminants. It is effective because of its large surface area, nanoscale dimensions, high density, and higher intrinsic reactivity of surface sites [5,9–12]. In recent years, there have been a few reports of using nZVI for removing heavy metal such as Pb^{2+}, Cu^{2+}, Co^{2+}, Ba^{2+}, and Cr^{+6} from wastewaters. The reports describe excellent uptake capabilities for various types of heavy metal ions [5,11,13–17]. However, nZVI use has caused to some problems such as high reactivity rates to surrounding media, floc formation, and loss of reactivity [13,18,19]. To overcome these problems, nZVI supported on kaolinite, zeolite, or bentonite has been effectively employed [5,6,10,11,20]. Another application has been nanoparticle coating on microbial cells [13,21–24]. Magnetically modified cells have been used for the removal of metals such as mercury, copper, cadmium, and chromium [13,21,22]. However, there is only a very limited number of papers describing magnetic modification of microbial cells. For this reason, this study investigated the potential of *S. cerevisiae* cells modified with nZVI (a magnetic biosorbent) to remove Ni(II) ions from aqueous solutions. In the first part of the study, *S. cerevisiae* cells modified with nZVI were synthesized and characterized. In the second part, Ni (II) removal properties were studied and possible removal mechanisms are discussed. The experiments were performed by varying solution pH, Ni(II) concentration, magnetic biosorbent amount, contact time, and Na^+ concentration. The magnetic biosorbent samples were characterized using FTIR, XRD, and SEM.

2. Materials and methods

2.1. Synthesis of S. cerevisiae cells modified with nZVI

S. cerevisiae yeast used in this study was waste granule yeast provided by the Turkey-Izmir Pakmaya Factory. Before use, the yeast was washed with distilled water and dried at 60°C in oven. The synthesis of magnetic biosorbent following the borohydride reduction method [5,25,26]. $FeCl_2{\cdot}4H_2O$ and $NaBH_4$ were used as iron and borohydride sources, respectively. Magnetic biosorbent was synthesized so that the Fe:*S. cerevisiae* ratio was 1:1. This was done by dissolving 5.34 g $FeCl_2{\cdot}4H_2O$ into a 4/L ethanol/distilled water mixture (total 30 mL solution), adding 1.5 g *S. cerevisiae* and mixing the solution with an ultrasonic shaker. On the other hand, 1 M $NaBH_4$ solution (100 mL) was prepared, which was added drop wise to the Fe(II)–*S.cerevisiae* solution and then shaken in a ultrasonic shaker. Black solid particle immediately appeared after adding the first drop of the $NaBH_4$ solution. The mixture was then left stirring for more than 10 min. To separate the magnetic biosorbent from the liquid phase, vacuum filtration was used. At this stage, solid particles were washed at least three times with absolute ethanol (25 mL). Finally, the synthesized material was oven-dried overnight at 50°C [5]. The reduction of iron ions by borohydride ions can be represented by reaction [5].

$$Fe(H_2O)_6^{2+} + 2BH_4^- \rightarrow Fe^0 \downarrow + 2B(OH)_3 + 7H_2$$

Magnetic modification of biosorbents makes them suitable for removing heavy metals by magnetic separation techniques. Biosorbents exhibit magnetic properties when placed in a magnetic field, but retain no residual magnetism when removed from the magnetic field. They should form stable colloidal suspensions, and they should not sediment or aggregate in the absence of magnetic fields [23].

2.2. Batch experiments

A Ni(II) stock solution (1,000 mg/L) was prepared using $NiCl_2{\cdot}6H_2O$ and distilled water. The batch experiments were carried out in 250 mL Erlenmeyer flasks containing 50 mL of Ni(II) solution. pH was adjusted with HCl and NaOH. Different amounts of magnetic biosorbent were added to Ni(II) solution. The suspension was shaken in temperature controlled shaker at 130 rpm and then centrifuged at 4,000 rpm for 5 min. The supernatant solutions were transferred to clean falcon tubes. The Ni(II) concentration in the supernatant was measured using an air-acetylene flame atomic absorption spectrometer (GBC Avanta R) at 351.5 nm wavelengths. Effects of solution pH (4–8), magnetic biosorbent amount (1–12 g/L), contact time (2.5–180 min), initial Ni(II) concentration (10–150 mg/L), and temperature (20–50°C) on Ni(II) biosorption onto magnetic biosorbent were investigated. The effect of Na^+ ions was investigated by changing the concentration of NaCl from 0.025 to 1 M and holding initial concentration of Ni(II) constant at 50 mg/L. Batch experimental conditions were given in Table 1. All experiments were conducted in duplicate and average results were reported.

The biosorption capacity (q_e, mg/g) and removal efficiency (%) were determined using Eqs. (1) and (2):

$$q_e = \frac{(C_o - C_e)V}{m} \quad (1)$$

$$\text{Removal efficiency } (\%) = \frac{C_o - C_e}{C_o} \times 100 \quad (2)$$

where C_o and C_e are the initial and the equilibrium Ni (II) concentration (mg/L), V is the volume of solution (L), and m is the amount of magnetic biosorbent (g).

3. Results and discussion

3.1. Characterization of magnetic biosorbent

XRD patterns of nZVI (a) and magnetic biosorbent before (b) and after Ni(II) removal (c) are presented in Fig. 1(a)–(c). XRD peaks at 2-theta 44.9˚C in nZVI and magnetic biosorbent is indicated the presence of Fe^0. This shows that Fe^0 was supported on the *S. cerevisiae* [12,27–29]. Additionally, iron oxides (Fe_3O_4/γ-Fe_2O_3 and FeO) are present as a thin layer on the nZVI. The peaks at 30° and 33° are associated with Fe_3O_4/γ-Fe_2O_3 and FeO, respectively. The peak at 30˚ was observed in magnetic biosorbent [11]. In XRD patterns, different peaks of magnetic biosorbent were observed due to the amorphous structure of *S. cerevisiae* [30].

FTIR spectrum for nZVI, magnetic biosorbent, and Ni-magnetic biosorbent were scanned for 4,000–450 cm^{-1} (Fig. 1(d)–(f)). The wide band around 3,300 cm^{-1} in composites is assigned to the stretching of O–H group of macromolecular association. This is because iron oxide surfaces are rapidly covered with hydroxyl groups in solution [13]. For the magnetic biosorbent, the band at 2,925 cm^{-1} was assigned to –CH_2– stretching and the weak band at 2,843 cm^{-1} to alkane C–H, which can be considered to be the characteristic peak of *S. cerevisiae* structure [30,31]. Strong bands at <900 cm^{-1} in the nZVI may be attributable in part to iron oxides on the surface. These bands are weaker in the magnetic biosorbent due to reduce oxidation of *S. cerevisiae*-supported Fe^0. This may be due to reduced Fe hydroxide formation [6]. The presence of these peaks in FTIR spectra confirmed that *S. cerevisiae* cells were successfully coated with iron particles. The 1,336–1,128 cm^{-1} peaks in the nZVI reflect the ethanol used in preparing the composites. However, these peaks were not observed in the FTIR pattern of the magnetic biosorbent. The FTIR spectra of magnetic biosorbent show different peaks after Ni(II) removal. There are some functional groups on the cell wall of the *S. cerevisiae* for binding of Ni(II) ions. The FTIR spectra of magnetic biosorbent after Ni(II) removal indicate active functional groups of O–H stretching (3,600–3,200 cm^{-1}), CH_2 stretching (2,900–2,800 cm^{-1}), –C=O, C–N (amide I) stretching (around 1,600 cm^{-1}), and C–O stretching (1,300–1,000 cm^{-1}) [30]. In addition,

Table 1
Batch experimental conditions

Experimental conditions						
Set	Aim of experiment	Solution pH	Initial Ni(II) conc. (mg/L)	Magnetic biosorbent dosage (g/L)	Contact time (min)	Temperature
1	Effect of solution pH	4–8	50	5.0	180	Room temperature (20˚C)
2	Effect of magnetic biosorbent dosage	5	50	1–12	180	Room temperature (20˚C)
3	Adsorption kinetics	5	50	3.0	2.5–180	Room temperature (20˚C)
4	Adsorption equilibrium tests	5	10–150	3.0	180	Room temperature (20˚C)
5	Effect of temperature	5	50	3.0	180	20–50˚C
6	Effect of ionic strength (0.025–1.00 M NaCl)	5	50	3.0	180	Room temperature (20˚C)

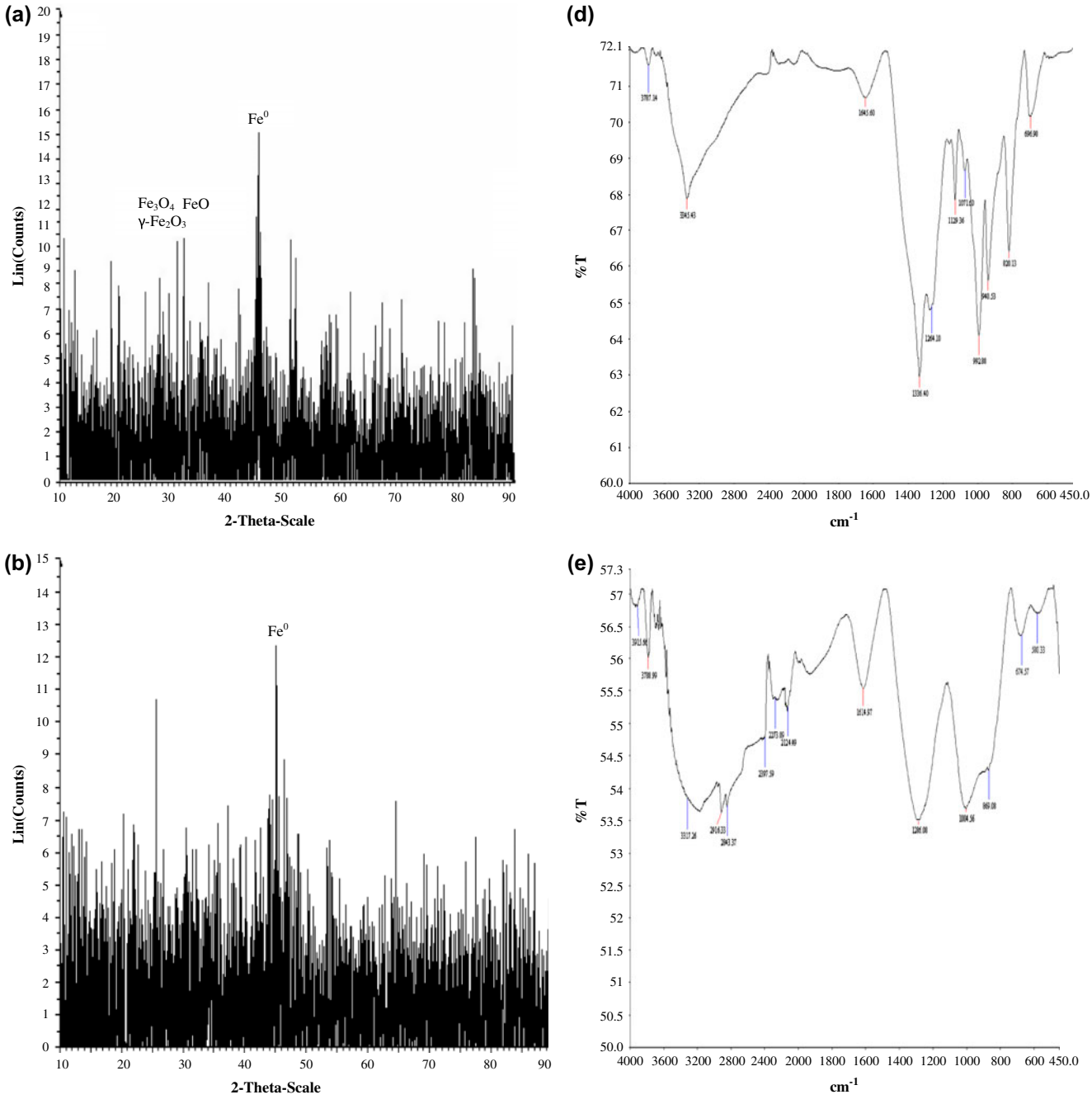

Fig. 1. XRD (a,b,c) and FTIR (d,e,f) patterns of nZVI (a), magnetic biosorbent (b) and Ni-magnetic biosorbent (c), nZVI (d), magnetic biosorbent (e), and Ni-magnetic biosorbent (f).

alkynes (C≡C) or nitriles (–C≡N) (2,400–2,100 cm^{-1}) stretching is lost. The stretching at 1,000 cm^{-1} (carboxylic acid) and <900 cm^{-1} in the Ni(II)-magnetic biosorbent is stronger than the magnetic biosorbent without Ni(II). All these data show that the Ni(II) uptake is formed by functional groups of the polysaccharides on the peptidoglycan layer on the *S. cerevisiae* cell surface and surface complexation the outer shell of nZVI [30,32].

According to SEM images, the aggregation of nZVI resulted in less reaction activity of nZVI (Fig. 2) [3]. Magnetically modified yeast cells surfaces are quite rough, providing a large exposed surface area for biosorption of Ni(II) ions [21].

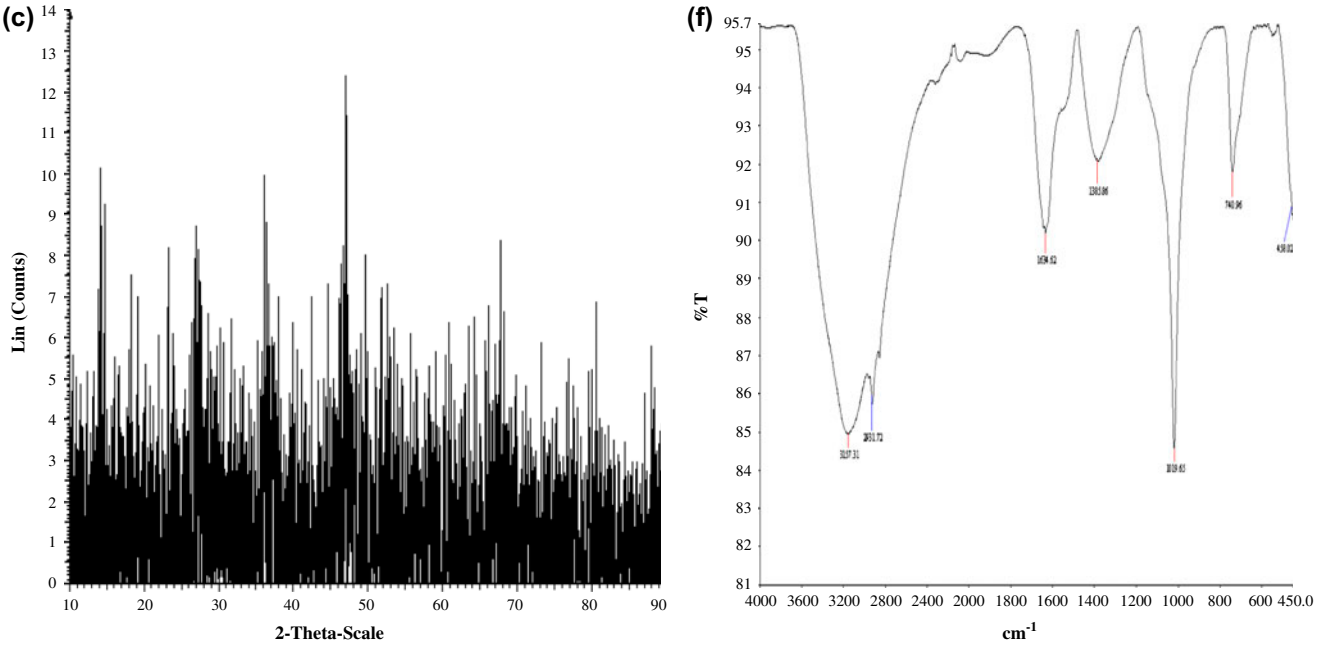

Fig. 1. (*Continued*).

In addition, the specific surface area, total pore volume, and mean pore diameter of nZVI magnetic biosorbent were 10.13 m^2/g, 0.10 cm^3/g, 40.01 nm and 21.01 m^2/g, 0.04 cm^3/g, 7.81 nm, respectively. The specific surface area of magnetic biosorbent was two times larger than nZVI alone (10.13 m^2/g).

3.2. Effect of solution pH

The pH value of the aqueous solution plays an important role in the removal process because it affects the different hydroxyl forms ($Ni(OH)^+$, $Ni(OH)_2$, and $Ni(OH)_3^-$) of Ni(II), the surface characteristics of the biosorbent and the chemical properties of the biosorbent during reaction [31,33–35]. At higher pH values ($pH \geq 8$), the removal mechanism is via both biosorption and metal ion precipitation as hydroxides. At lower values of pH, the surface charge of the solid may be too positive and nickel cation biosorption unfavorable, and hydrogen ions may compete strongly with nickel ions for the active sites of magnetic biosorbent and biosorption may be reduced [3]. In addition, the adsorption properties of oxide and oxyhydroxide groups on the shell of iron nanoparticles are strongly affected by solution pH [5,36]. If the pH is basic, the oxide surface becomes negatively charged and therefore surface complexation reactions increase. The pH is important in determining the thickness of the double layer at the interface between the oxide surface and solution. If the pH is acidic, the double layer becomes thicker due to repulsive forces between the positively charged surface and the cations, thus decreasing reaction possibilities between the adsorbate and the surface [5]. Therefore, the effect of initial pH on Ni(II) biosorption was studied by varying the pH from 4 to 8 (Fig. 3(a)). Varying the initial pH value had a small effect on Ni(II) removal efficiency. The removal efficiency was 77% at initial pH 4, while the removal efficiency was 80% at initial pH 5 and 6, 81% at initial pH 7 and 8. Hence, different pH values have a minimal effect on the surface charge of yeast [6,37]. Removal efficiency was no significantly different between pH 5 and pH 8. Therefore, pH 5 was selected as the optimum pH value for the Ni(II) solution. In subsequent experiments, the predominant species was Ni(II) at pH 5.

3.3. Effect of magnetic biosorbent amount

The effect of magnetic biosorbent amount on Ni(II) biosorption is shown in Fig. 3(b). It is clear that Ni(II) removal increased from 69 to 83% by increasing the amount of magnetic biosorbent from 1 to 12 g/L. The increase of Ni(II) removal was due to an increase in biosorptive and active sites of the magnetic biosorbent [10]. The optimum amount of magnetic biosorbent for further experiments of Ni(II) removal was selected as 3 g/L.

3.4. Adsorption isotherms

Isotherm studies were carried out by varying the initial Ni(II) ion concentrations from 10 to 150 mg/L at

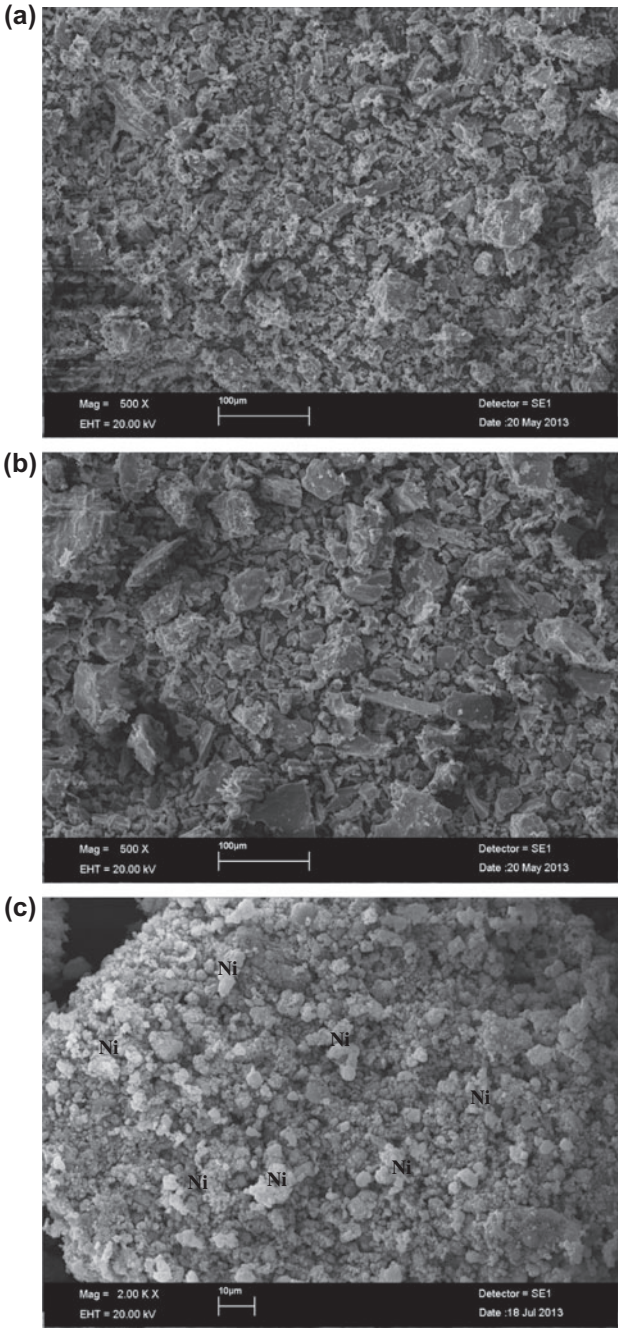

Fig. 2. SEM images of nZVI (a), magnetic biosorbent (b), and Ni-magnetic biosorbent (c).

pH 5 and room temperature. The initial concentration of metal ions provides an important driving force to overcome all mass transfer resistance of metal ions between aqueous and bulk phases. Therefore, initial Ni (II) ion concentration was selected based on Ni(II) concentrations in wastewaters and literature studies. Analysis of equilibrium data is important for developing an equation that accurately represents the results that can be used for design purposes [3]. The adsorption equilibrium is described by the Langmuir, Freundlich, Dubinin–Radushkevich (D–R), and Temkin adsorption models, which are the most widely used isotherm models. All isotherm models parameters were calculated using non-linear regression in the Sigmaplot 11 program.

Eq. (3) of the Langmuir model is given below [38,39]:

$$q_e = \frac{Q_m b C_e}{1 + bC_e} \tag{3}$$

where Q_m is the maximum adsorption capacity (mg/g) and b is the Langmuir constant that relates to the energy of adsorption (L/mg). In order to find out the feasibility of the isotherm, the essential feature of the Langmuir isotherm can be expressed in terms of a dimensionless constant separation factor or equilibrium parameter (R_L). R_L is given by Eq. (4) [38,40]:

$$R_L = \frac{1}{1 + bC_o} \tag{4}$$

The value of R_L indicates the type of the isotherm to be irreversible ($R_L = 0$), favorable ($0 < R_L > 1$), linear ($R_L = 1$), or unfavorable ($R_L > 1$).

The Freundlich isotherm is derived to model multilayer adsorption and adsorption on heterogeneous surfaces. The linear form of Freundlich isotherm is given by Eq. (5) [38,41]:

$$q_e = k_F C_e^{\frac{1}{n}} \tag{5}$$

where k_F is the Freundlich constant related to adsorption capacity (L/g) and n is adsorption intensity. The $1/n$ values were between 0 and 1 indicating that adsorption was favorable under these conditions.

D–R isotherm is more general than the Langmuir isotherm. It was applied to identify adsorption processes as physical or chemical. The D–R isotherm Eq. (6) is expressed as follows [42]:

$$q_e = q_{D-R} e^{\beta \varepsilon^2} \tag{6}$$

where q_e is the amount of pollution adsorbed on the adsorbent at equilibrium (mol/g), q_{D-R} is the maximum adsorption capacity (mol/g), β is a coefficient related to the mean free energy of adsorption (mol^2/J^2), and ε is the Polanyi potential (J/mol) given

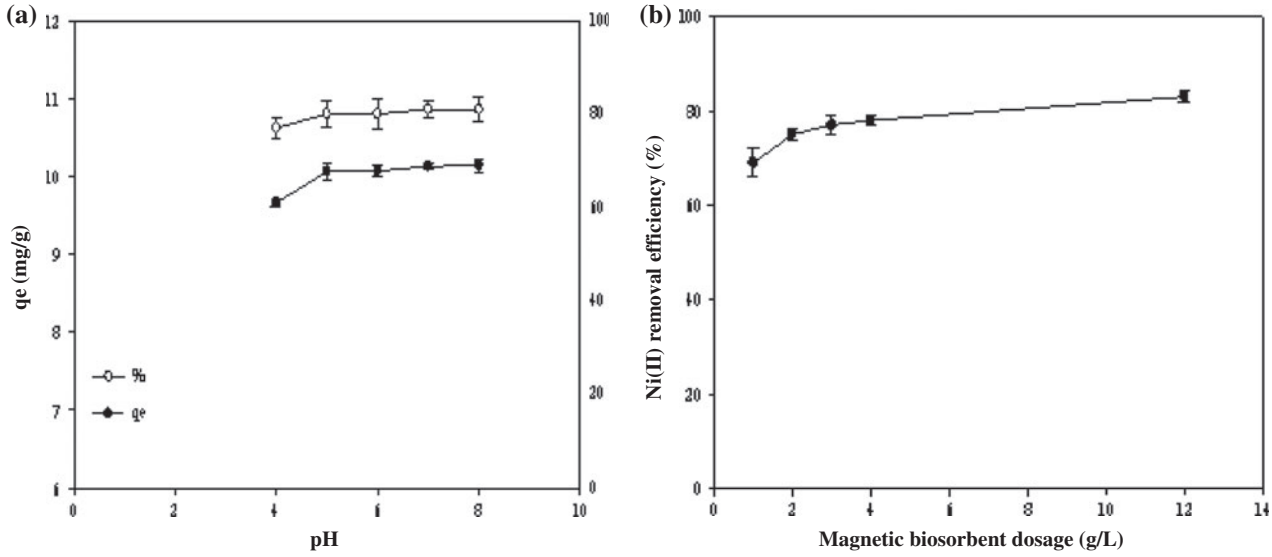

Fig. 3. Effect of pH and biosorbent dosage on Ni(II) removal. Data points and error bars represent the average of double samples and standard deviation, respectively.

with $\varepsilon = RT \ln(1 + 1/C_e)$. The mean free energy E (kJ/mol) is then derived from (Eq. (7)):

$$E = \frac{1}{\sqrt{-2\beta}} \tag{7}$$

The Temkin isotherm is given by the following equation. K_T and b_T are called binding (L/mg) and Temkin constants (g kJ/mg mol) calculated from the slope and the intercept of the linear plot of q_e vs. ln C_e (Eq. (8)) [43].

$$q_e = \frac{RT}{b_T} \ln(K_T C_e) \tag{8}$$

The results of fitting these models are shown in Fig. 4(a)–(c). Isotherm constants were calculated from the isotherm models and the correlation coefficients are given in Table 2.

Ni(II) biosorption is fitted excellently to both Langmuir and Freundlich isotherms (R^2 0.998). The applicability of both Langmuir and Freundlich isotherms to the biosorption of Ni(II) onto magnetic biosorbent shows that biosorption occurred at two specific localized sites on a homogeneous surface by the monolayer formation of an adsorbate. Firstly, the biosorbent surface; and secondly, on a reversible heterogeneous surface consisting of different biosorption energies in the biosorption sites [10,44,45]. The Langmuir model shows that the maximum biosorption capacity (Q_m) for magnetic biosorbent was 54.23 mg/g. This value is approximately 2.5 times higher than unmodified *S. cerevisiae* (21.39 mg/g) [30]. The Q_m values of various adsorbents for Ni(II) ions are presented in Table 3 [3,4,30,35,46].

Moreover, the $1/n$ heterogeneity value for magnetic biosorbent was between 0 and 1 indicating that the Ni(II) biosorption was favorable under these conditions. The calculated R_L values also range between 0 and 1, indicating that the Ni(II) biosorption onto the magnetic biosorbent is favorable and suitable over a range of initial Ni(II) concentrations [10,44]. At high Ni(II) concentrations, the decrease in R_L values indicated a less significant role in biosorption. However, the higher values of Ni(II) removal with higher Ni(II) concentration showed that the cell associated Fe^0/Fe_3O_4 composites played a primary role in the uptake mechanism (Table 4).

The Freundlich constant (k_F) for the unmodified *S. cerevisiae* cells is reported to be 0.84 L/g [30]. The presence of nanocomposites on the *S. cerevisiae* cell surface increased k_F values to 2.681 L/g. The high values of these coefficients for *S. cerevisiae* cells modified with nZVI indicate enhanced specific uptake [47].

The mean free energy (E, kJ/mol) values calculated from the D–R isotherm model were between 8 and 16 kJ/mol. The biosorption process was physical via ion exchange and/or surface complexation under the influence of coulomb forces [48,49].

According to the Temkin isotherm model, K_T and b_T values were −3.93 and 308.53, respectively.

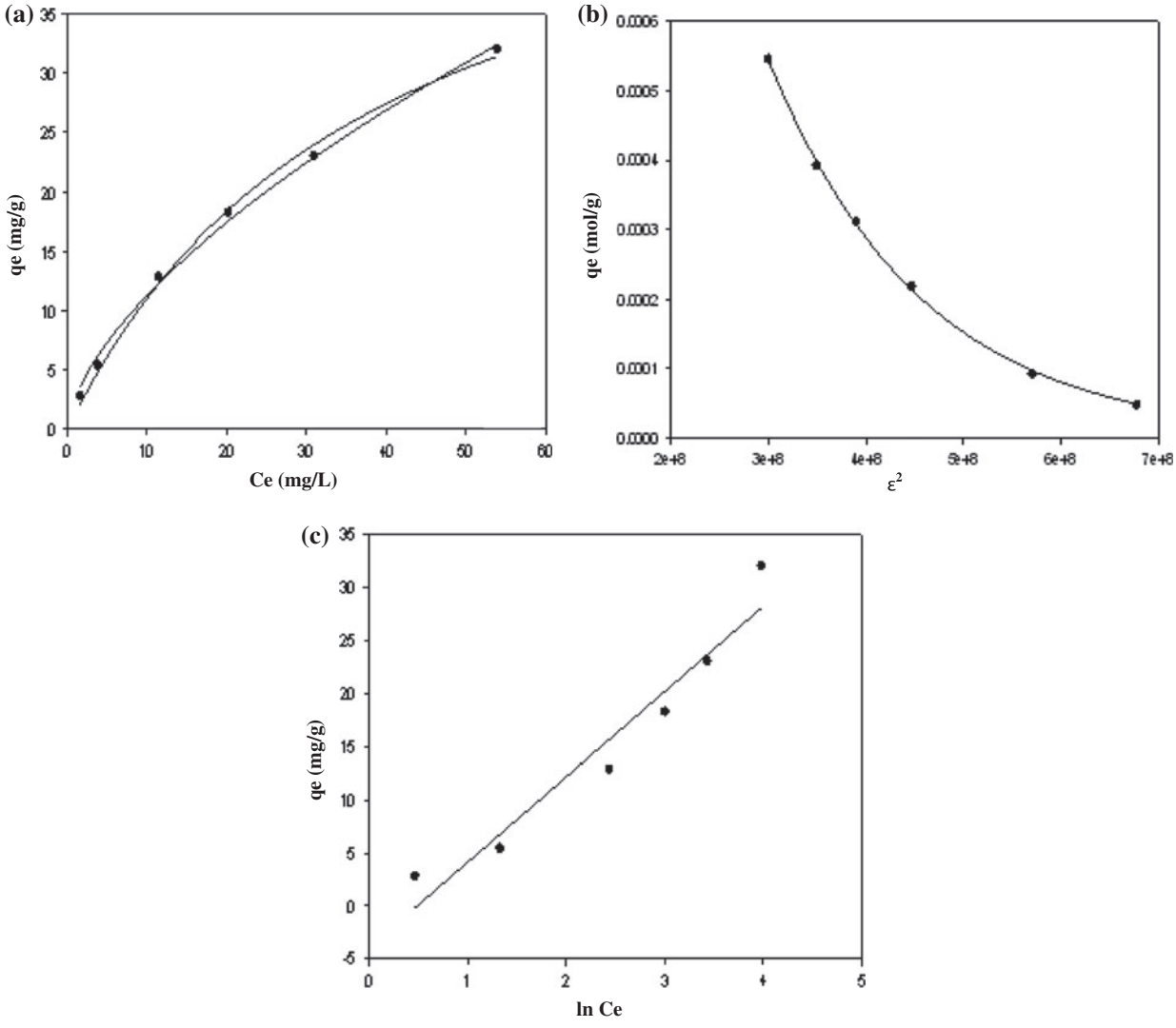

Fig. 4. Adsorption isotherms of Ni(II) onto *S. cerevisiae*-nZVI; Langmuir and Freundlich (a), D–R (b), and Temkin isotherm model (c).

Table 2
Langmuir, Freundlich, and D–R adsorption isotherm parameters of Ni(II) removal by magnetic biosorbent

	Langmuir				Freundlich		
Magnetic biosorbent	Q_m (mg/g)	b (L/mg)	R^2		k_F (L/g)	$1/n$	R^2
	54.23	0.0256	0.998		2.681	0.62	0.998
	D–R				Temkin		
	q_{D-R}(mol/g)	E (kJ/mol)	β (mol^2/J^2)	R^2	b_T (g kJ/mg mol)	K_T (L/mg)	R^2
	0.0037	8.87	$6.36.10^{-9}$	0.999	308.53	−3.93	0.968

Table 3
Maximum adsorption capacity (Q_m) of various adsorbents for Ni(II)

Adsorbent	Q_m (mg/g)	Reference
S. cerevisiae-nZVI	54.23	This study
Sugarcane bagasse	1.34	[3]
Spirogyra sp.	11.95	[4]
S. cerevisiae	21.39	[30]
Baker's yeast	11.40	[35]
Dye groundnut shells	7.49	[46]

Table 4
Equilibrium biosorption capacities and R_L values for magnetic biosorbent

C_o (mg/L)	q_e (mg/g)	R_L
10	2.80	0.80
20	5.40	0.66
50	12.83	0.44
75	18.25	0.34
100	23.00	0.28
150	32.00	0.21

3.5. Reduction kinetics

The effect of contact time on Ni(II) removal was investigated for 2.5–180 min with an the initial Ni(II) ion concentration of 50 mg/L (Fig. 5), and kinetics were calculated. As expected, magnetic biosorbent showed strong biosorption during the first 15 min (external surface biosorption) and after 90 min (internal surface biosorption), then the biosorption reached equilibrium.

The kinetics of Ni(II) removal was analyzed using the pseudo-first-order Lagergren, pseudo-second-order model, and intraparticle diffusion model.

The pseudo-first-order kinetic model is expressed as [38,50]:

$$\log(q_e - q_t) = \log\ q_e - \frac{k_1}{2.303}t \tag{9}$$

The pseudo-second-order kinetic model is given as [51]:

$$\frac{t}{q_t} = \frac{1}{k_2(q_e)^2} + \frac{t}{q_e} \tag{10}$$

The initial sorption rate h (mg/g min):

$$h = k_2 q_e^2 \tag{11}$$

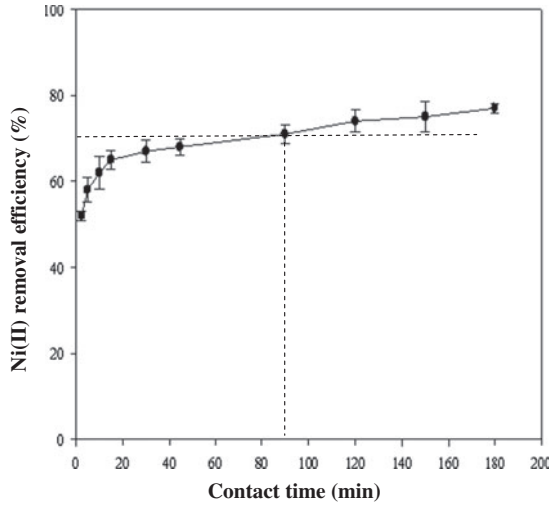

Fig. 5. Effect of contact time on Ni(II) removal. Data points and error bars represent the average of double samples and standard deviation, respectively (C_o 50 mg/L, X_o 3 g/L, pH 5, and room temperature).

The intraparticle diffusion model plays an important role in the extent of biosorption and can be described by the following equation [52,53]:

$$q_t = k_d t^{0.5} + I \tag{12}$$

where q_e and q_t (mg/g) are the amounts of Ni(II) ions adsorbed on the adsorbent at equilibrium and time t (min), I is the intercept and k_1 (1/min), k_2 (g/mg min), and k_d (mg/g $\text{min}^{0.5}$) are the rate constant of pseudo-first-order kinetic model, pseudo-second-order kinetic model, and intraparticle diffusion model, respectively. Table 5 shows the correlation coefficients (k_1, k_2, k_d) and equilibrium biosorption capacities ($q_{e,\text{teo}}$) in these models (pseudo-first-order kinetic model, pseudo-second-order kinetic model, and intraparticle diffusion model) and initial sorption rate (h).

The correlation coefficient (R^2) agrees well with experimental $q_{e\text{exp}}$ and calculated $q_{e\text{cal}}$ values. The pseudo-second-order kinetic model is represented by the biosorption kinetics. In this case, the biosorption rate-limiting step may be chemisorptions because Ni (II) removal probably occurs via surface complexation reactions at specific biosorption sites [54–56]. The plot of the intraparticle diffusion model can be evaluated in two linear parts. The first part reflects rapid initial uptake via boundary layer effects until external surfaces are covered, followed by the second part, intraparticle diffusion [49].

Table 5
Kinetic parameters of the Ni(II) removal by magnetic biosorbent

	Pseudo-first-order			Pseudo-second-order				Intraparticle		
$q_{e\exp}$	k_1 (1/min)	$q_{e\text{cal}}$	R^2	$q_{e\text{cal}}$	k_2 (g/mg min)	h (mg/g min)	R^2	k_d (mg/g min$^{0.5}$)	I	R^2
12.83	0.014	3.13	0.955	12.82	0.023	3.78	0.998	0.288	9.48	0.897

3.6. Thermodynamic parameters

The standard free energy change (ΔG°), standard enthalpy change (ΔH°), and standard entropy change (ΔS°) were calculated using the following equations [57,58]:

$$\Delta G^\circ = -RT \ln K_d \quad (13)$$

$$\ln K_d = \frac{\Delta S^\circ}{R} - \frac{\Delta H^\circ}{RT} \quad (14)$$

$$\Delta G^\circ = \Delta H^\circ - T\Delta S^\circ \quad (15)$$

where ΔG° is the standard free energy change (kJ/mol), ΔH° is the standard enthalpy change (kJ/mol), and ΔS° is the standard entropy change (kJ/mol K); R is the universal gas constant (8.314 J/mol K), T is the temperature (K), and K_d (q_e/C_e) is the equilibrium constant. The values of ΔH° and ΔS° in the biosorption process were determined from a slope and intercept of the plot of ln K_d vs. $1/T$, respectively. The calculated values of ΔH°, ΔS°, and ΔG° are shown in Table 6.

The value of ΔH° was positive, indicating that the biosorption of Ni(II) was endothermic in nature. Negative values of ΔG° indicate that Ni(II) biosorption onto the magnetic biosorbent was spontaneous and feasible [10,59]. In addition, possible Ni(II) removal involving both physical and chemical biosorption was suggested. It is reported that the value of ΔH° for absolute physical biosorption is less than 20 kJ/mol, while chemisorptions are in the range of 80–200 kJ/mol [10,60]. The positive value of ΔS shows the increase in randomness at the solid–liquid interface during the biosorption process [61].

Table 6
Thermodynamic parameters obtained for adsorption of Ni(II) removal by magnetic biosorbent

Parameters	Temperature (K)	Magnetic biosorbent
ΔH° (kJ/mol)		16.05
ΔS° (kJ/mol K)		112.41
ΔG° (kJ/mol)	298	−17.39
	308	−18.12
	318	−19.37
	328	−20.67

3.7. Effect of ionic strength on biosorption

Effect of ionic strength was investigated at different concentrations of NaCl. Biosorption capacity decreased with the addition of NaCl (Fig. 6).

This can be explained by the competition between Ni(II) ions and Na^+ ions for biosorption to the same sites of the magnetic biosorbent. This result also supports the general result that electrostatic attraction decreases with increasing ionic strength [62].

3.8. Mechanism of Ni(II) removal by S. cerevisiae cells modified with nZVI

Ni(II) removal by the *S. cerevisiae* cells modified with nZVI may be realized via five mechanisms: (a) direct reduction of Ni(II) with the oxidation of Fe^0 to Fe^{3+} in the magnetic biosorbent, (b) surface complexation via hydroxyl groups on the shell of nZVI, (c) biosorption of Ni(II) ions by functional groups onto the yeast cells, (d)

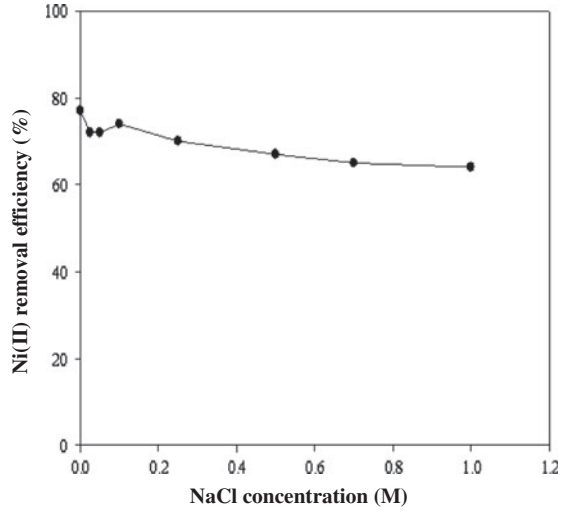

Fig. 6. Effect of ionic strength on Ni(II) removal by magnetic biosorbent (C_o 50 mg/L, pH 5, X_o 3 g/L, contact time 3 h, and room temperature).

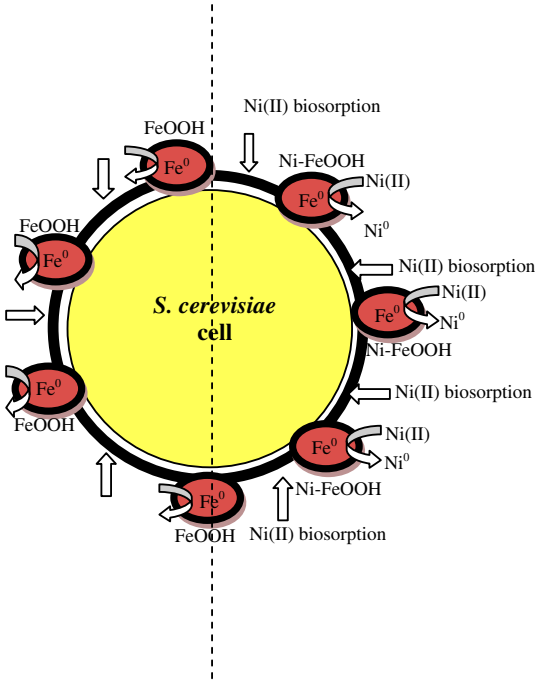

Fig. 7. Proposed mechanism for Ni(II) removal by *S. cerevisiae* cells modified with nZVI.

translocation of nickel across the oxide shell accompanied by further breaking of Ni−O bonds, and (e) diffusion into the Fe^0 core and yeast cell wall [63,64]. A schematic representation of these mechanisms is given in Fig. 7.

These possible reactions can be summarized as follows:

$$Fe^0 + Ni^{2+} + 2H^+ \rightarrow Fe^{2+} + Ni^0 + H_2O + 2e^- \quad \text{(oxidation in acidic solution)} \tag{16}$$

$$Fe^0 + Ni^{2+} + 2H_2O \rightarrow Fe^{2+} + Ni^0 + 2OH^- + 2e^- \quad \text{(oxidation in basic solution)} \tag{17}$$

$$Ni^0 + Fe^{2+} + 2H^+ + 1/2O_2 \rightarrow Fe^{3+} + Ni + H_2O \tag{18}$$

$$xNi + (1-x)Fe^{3+} + OH \rightarrow Ni_x(OH)_2 \downarrow + Fe_{(1-x)}(OH)_3 \downarrow \text{(reduction)} \tag{19}$$

$$Ni^{2+} + S.\ cerevisiae\ \text{cell} \rightarrow Ni^{2+} - S.\ cerevisiae\ \text{cell (biosorption)} \tag{20}$$

4. Conclusions

This study synthesized *S. cerevisiae* modified with nZVI. A variety of techniques such as XRD, FTIR, and SEM confirmed the modification. Magnetically modified yeast cells were used as an biosorbent for Ni(II) removal from aqueous solutions. The *S. cerevisiae* modified with nZVI were 2.5 times more effective in removing Ni(II) ions than unmodified *S. cerevisiae* cells. XRD, FTIR, and SEM analyses demonstrated that the surface area of the magnetic biosorbent has a quite rough surface, which is a good feature for biosorption. The maximum biosorption capacity was found to be 54.23 mg/g (pH 5.0, magnetic biosorbent amount 3 g/L, and contact time 3 h). Biosorption kinetics were a good fit to the pseudo-second-order kinetic model. The Ni(II) biosorption onto the magnetic biosorbent was found to be endothermic and spontaneous.

Finally, *S. cerevisiae* modified with nZVI showed high removal efficiency (77%). This study contributes to understanding the potential use of magnetically modified cells for wastewater treatment.

Abbreviations

nZVI	—	nano zero-valent iron
magnetic biosorbent	—	nZVI-modified cells of *S. cerevisiae*
D–R	—	Dubinin–Radushkevich
ΔG°	—	the standard free energy change
ΔH°	—	standard enthalpy change
ΔS°	—	standard entropy change

References

[1] U. Acıkel, M. Ersan, Acid phosphatase production by Rhizopus delemar: A role played in the Ni(II) bioaccumulation process, J. Hazard. Mater. 184 (2010) 632–639.
[2] J.W. Patterson, Wastewater Treatment Technology, Ann Arbor Science, New York, NY, 1977.
[3] I. Aloma, M.A. Martín-Lara, I.L. Rodríguez, G. Blázquez, M. Calero, Removal of nickel (II) ions from aqueous solutions by biosorption on sugarcane bagasse, J. Tai. Inst. Chem. Eng. 43 (2012) 275–281.
[4] U.A Guler, M. Sarioglu, Single and binary biosorption of Cu(II), Ni(II) and methylene blue by raw and pretreated *Spirogyra sp.*: Equilibrium and kinetic modeling, J. Environ. Chem. Eng. 1 (2013) 369–377.
[5] C. Uzum, T. Shahwan, A.E. Eroğlu, K.R. Hallam, I. Scott, Lieberwirth synthesis and characterization of kaolinite-supported zero-valent iron nanoparticles and their application for the removal of aqueous Cu^{2+} and Co^{2+} ions, Appl. Clay Sci. 43 (2009) 172–181.

[6] S.A. Kim, S.K. Kannan, K.J. Lee, P.Y.J. Park, J. Shea, W.H. Lee, H.M. Kim, B.T. Oha, Removal of Pb(II) from aqueous solution by a zeolite–nanoscale zero-valent iron composite, Chem. Eng. J. 217 (2013) 54–60.
[7] P.K. Malik, S.K. Saha, Oxidation of direct dyes with hydrogen peroxide using ferrous ion as catalyst, Sep. Purif. Technol. 31 (2003) 241–250.
[8] M.K. Mondal, Removal of Pb(II) ions from aqueous solution using activated tea waste: Adsorption on a fixed-bed column, J. Environ. Manage. 90 (2009) 3266–3271.
[9] Z. Fang, J. Chen, X. Qiu, X. Qiu, W. Cheng, L. Zhu, Effective removal of antibiotic metronidazole from water by nanoscale zero-valent iron particles, Desalination 268 (2011) 60–67.
[10] Z. Chen, T. Wang, X. Jin, Z. Chen, M. Megharaj, R. Naidub, Multifunctional kaolinite-supported nanoscale zero-valent iron used for the adsorption and degradation of crystal violet in aqueous solution, J. Colloid Interface Sci. 398 (2013) 59–66.
[11] X. Zhang, S. Lina, Z. Chen, M. Megharaj, R. Naidu, Kaolinite-supported nanoscale zero-valent iron for removal of Pb^{2+} from aqueous solution: Reactivity, characterization and mechanism, Water Res. 45 (2011) 3481–3488.
[12] J.T. Nurmi, P.G. Tratnyek, V. Sarathy, D.R. Baer, J.E. Amonette, K. Pecher, C. Wang, J.C. Linehan, D.W. Matson, R.L. Penn, M.D. Driessen, Characterization and properties of metallic iron nanoparticles: Spectroscopy, electrochemistry, and kinetics, Environ. Sci. Technol. 39 (2005) 1221–1230.
[13] A. Rao, A. Bankar, A.R. Kumar, S. Gosavi, S. Zinjarde, Removal of hexavalent chromium ions by *Yarrowia lipolytica* cells modified with phyto-inspired Fe^0/Fe_3O_4 nanoparticles, J. Contam. Hydrol. 146 (2013) 63–73.
[14] T.Y. Liu, L. Zhao, X. Tan, S.J. Liu, J.J. Li, Y. Qi, G.Z. Mao, Effects of physicochemical factors on Cr(VI) removal from leachate by zero-valent iron and alpha-Fe_2O_3 nanoparticles, Water Sci. Technol. 61 (2010) 2759–2767.
[15] R. Singh, V. Misra, R.P. Singh, Removal of hexavalent chromium from contaminated ground water using zero-valent iron nanoparticles, Environ. Monit. Assess. 184 (2012) 3643–3651.
[16] O. Celebi, C. Uzum, T. Shahwan, H.N. Erten, A radiotracer study of the adsorption behavior of aqueous Ba^{2+} ions on nanoparticles of zero-valent iron, J. Hazard. Mater. 148 (2007) 671–676.
[17] D. Karabelli, C. Uzum, T. Shahwan, A.E. Eroglu, T. Scott, K.R. Hallam, I. Lieberwirth, Batch removal of aqueous Cu^{2+} ions using nanoparticles of zero-valent iron: a study of the capacity and mechanism of uptake, Ind. Eng. Chem. Res. 47 (2008) 4758–4764.
[18] F. He, D. Zhao, Preparation and characterization of a new class of starch-stabilized bimetallic nanoparticles for degradation of chlorinated hydrocarbons in water, Environ. Sci. Technol. 39 (2005) 3314–3320.
[19] P. Yuan, M. Fan, D. Yang, H. He, D. Liu, A. Yuan, J.X. Zhu, T. Chen, Montmorillonite-supported magnetite nanoparticles for the removal of hexavalent chromium Cr(VI) from aqueous solutions, J. Hazard. Mater. 166 (2009) 821–829.
[20] L.N. Shi, X. Zhang, Z.L. Chen, Removal of Chromium (VI) from wastewater using bentonite-supported nanoscale zero-valent iron, Water Res. 45 (2011) 886–892.
[21] H. Yavuz, A. Denizli, H. Gungunes, M. Safarikova, I. Safarik, Biosorption of mercury on magnetically modified yeast cells, Sep. Purif. Technol. 52 (2006) 253–260.
[22] M. Patzak, P. Dostalek, R.V. Fogarty, I. Safarik, J.M. Tobin, Development of magnetic biosorbents for metal uptake, Biotechnol. Tech. 117 (1997) 483–487.
[23] I. Safarik, L.F.T. Rego, M. Borovska, E. Mosiniewicz-zablewska, F Weyda, M. Safarikova, New magnetically responsive yeast-based biosorbent for the efficient removal of water-soluble dyes, Enzyme Microb. Technol. 40 (2007) 1551–1556.
[24] I. Safarik, M. Safarikova, Magnetically modified microbial cells: A new type of magnetic adsorbents, Chin. Partic. 5 (2007) 19–25.
[25] C. Wang, W. Zhang, Synthesizing nanoscale iron particles for rapid and complete dechlorination of TCE and PCBs, Environ. Sci. Technol. 31 (1997) 2154–2156.
[26] W. Wang, Z. Jin, T. Li, H. Zhang, S. Gao, Preparation of spherical iron nanoclusters in ethanol–water solution for nitrate removal, Chemosphere 65 (2006) 1396–1404.
[27] H. Chen, H. Luoa, Y. Lana, T. Donga, B. Hua, Y. Wang, Removal of tetracycline from aqueous solutions using polyvinylpyrrolidone (PVP-K30) modified nanoscale zero valent iron, J. Hazard. Mater. 192 (2011) 44–53.
[28] S.R. Kanel, J.M. Grenche, H. Choi, Arsenic(V) removal from groundwater using nano scale zero-valent iron as a colloidal reactive barrier material, Environ. Sci. Technol. 40 (2006) 2045–2050.
[29] A.B.M. Giasuddin, S.R. Kanel, H. Choi, Adsorption of humic acid onto nanoscale zerovalent iron and its effect on arsenic removal, Environ. Sci. Technol. 41 (2007) 2022–2027.
[30] U.A. Guler, M. Sarioglu, Mono and binary component biosorption of Cu(II), Ni(II), and methylene blue onto raw and pretreated, *S. cerevisiae*: Equilibrium and kinetics, Desalin. Water Treat. 52 (2014) 4871–4888.
[31] Q. Peng, Y. Liu, G. Zeng, W. Xu, C. Yang, J. Zhang, Biosorption of copper(II) by immobilizing *Saccharomyces cerevisiae* on the surface of chitosan-coated magnetic nanoparticles from aqueous solution, J. Hazard. Mater. 177 (2010) 676–682.
[32] N. Efecan, T. Shahwan, A.E. Eroğlu, I. Lieberwirth, Characterization of the uptake of aqueous Ni^{2+} ions on nanoparticles of zero-valent iron, Desalination 249 (2009) 1048–1054.
[33] S.M. Nomanbhay, K. Palanisamy, Removal of heavy metal from industrial wastewater using chitosan coated oil palm shell charcoal, Electron. J. Biotechnol. 8 (2005) 43–53.
[34] M. Iqbal, R.G.J. Edyvan, Biosorption of lead, copper and zinc ions on loofa sponge immobilized biomass of *Phanerochaete chrysosporium*, Miner. Eng. 17 (2004) 217–223.
[35] A. Özer, E. Özer, Comparative study of the biosorption of Pb(II), Ni(II) and Cr(VI) ions onto *S. cerevisiae*: Determination of biosorption heats, J. Hazard. Mater. 100 (2003) 219–229.

[36] X.Q. Li, W.X. Zhang, Sequestration of metal cations with zerovalent iron nanoparticles a study with high resolution X-ray photoelectron spectroscopy (HR-XPS), J. Phys. Chem. C. 111 (2007) 6939–6946.
[37] A. Ponizovsky, C.D. Tsadilas, Lead(II) retention by alfisol and clinoptilolite: Cation balance and pH effect, Geoderma 115 (2003) 303–312.
[38] Y. Wang, N. Chen, W. Wei, J. Cui, Z. Wei, Enhanced adsorption of fluoride from aqueous solution onto nanosized hydroxyapatite by low-molecular-weight organic acids, Desalination 276 (2011) 161–168.
[39] I. Langmuir, The dissociation of hydrogen into atoms. III. The mechanism of the reaction, J. Am. Chem. Soc. 38 (1916) 1145–1156.
[40] T.W. Webi, R.K. Chakravort, Pore and solid diffusion models for fixed-bed adsorbents, Aiche J. 20 (1974) 228–238.
[41] H.M.F. Freundlich, Über die adsorption in lösungen, J. Phys. Chem. 57 (1906) 385–470.
[42] V.B.H. Dang, H.D. Doan, T. Dang-Vu, A. Lohi, Equilibrium and kinetics of biosorption of cadmium(II) and copper(II) ions by wheat straw, Bioresour. Technol. 100 (2009) 211–219.
[43] N. Barka, M. Abdennouri, M. El Makhfouk, Removal of methylene blue and Eriochrome Black T from aqueous solutions by biosorption on *Scolymus hispanicus L.*: Kinetics, equilibrium and thermodynamics, J. Tai. Inst. Chem. Eng. 42 (2011) 320–326.
[44] A.S. Özcan, Ö. Gök, A. Özcan, Adsorption of lead(II) ions onto 8-hydroxy quinoline-immobilized bentonite, J. Hazard. Mater. 161 (2009) 499–509.
[45] X.G. Luo, L. Zhang, High effective adsorption of organic dyes on magnetic cellulose beads entrapping activated carbon, J. Hazard. Mater. 171 (2009) 340–347.
[46] S.R. Shukla, R.S. Pai, Adsorption of Cu(II), nickel(II) and Zn(II) on dye loaded groundnut shells and sawdust, Sep. Purif. Technol. 43 (2005) 1–8.
[47] P.S. Pimprikar, S.S. Joshi, A.R. Kumar, S.S. Zinjarde, S.K. Kulkarni, Influence of biomass and gold salt concentration on nanoparticle synthesis by the tropical marine yeast *Yarrowia lipolytica* NCIM 3589, Colloids Surf., B 74 (2009) 309–316.
[48] D. Baybas, U. Ulusoy, nPolyacrylamide–hydroxyapatite composite: Preparation, characterization and adsorptive features for uranium and thorium, J. Solid State Chem. 194 (2012) 1–8.
[49] R. Akkaya, U. Ulusoy, Adsorptive features of chitosan entrapped in polyacrylamide hydrogel for Pb^{2+}, UO_2^{2+}, and Th^{4+}, J. Hazard. Mater. 151 (2008) 380–388.
[50] S. Lagergren, About the theory of so-called adsorption of soluble substances, K. Sven. Vetenskapsakad. Handl. 24 (1898) 1–39.
[51] G. Crini, H.N. Peindy, F. Gimbert, C. Robert, Removal of CI basic green 4 (malachite green) from aqueous solutions by adsorption using cyclodextrin based adsorbent: Kinetic and equilibrium studies, Sep. Purif. Technol. 53 (2007) 97–110.
[52] N. Gupta, A.K. Kushwaha, M.C. Chattopadhyaya, Adsorptive removal of Pb^{2+}, Co^{2+} and Ni^{2+} by hydroxyapatite/chitosan composite from aqueous solution, J. Tai. Inst. Chem. Eng. 43 (2012) 125–131.
[53] W.J. Weber Jr., J.C. Morris, Kinetics of adsorption on carbon from solution, J. Sanit. Eng. Div. Asce. 89 (1963) 31–59.
[54] Y. Zhao, X. Gu, S. Gao, J. Geng, X. Wang, Adsorption of tetracycline (TC) onto montmorillonite: Cations and humic acid effects, Geoderma 183 (2012) 12–18.
[55] G. Asgari, B. Roshani, G. Ghanizadeh, The investigation of kinetic and isotherm of fluoride adsorption onto functionalize pumice stone, J. Hazard. Mater. 17 (2012) 123–132.
[56] A. Behnamfard, M.M. Salarirad, Equilibrium and kinetic studies on free cyanide adsorption from aqueous solution by activated carbon, J. Hazard. Mater. 170 (2009) 127–133.
[57] E.I. Unuabonah, K.O. Adebowale, B.I. Olu-Owolabi, Kinetic and thermodynamic studies of the adsorption of lead (II) ions onto phosphate-modified kaolinite clay, J. Hazard. Mater. 144 (2007) 386–395.
[58] A. Sari, M. Tuzen, M. Soylak, Adsorption of Pb(II) and Cr(III) from aqueous solution on Celtek clay, J. Hazard. Mater. 144 (2007) 41–46.
[59] M. Ersan, E. Bagda, E. Bagda, Investigation of kinetic and thermodynamic characteristics of removal of tetracycline with sponge like, tannin based cryogels, Colloids Surf., B 104 (2013) 75–82.
[60] Q. Li, Q.Y. Yue, Y. Su, B.Y. Gao, H.J. Sun, Equilibrium, thermodynamics and process design to minimize adsorbent amount for the adsorption of acid dyes onto cationic polymer-loaded bentonite, Chem. Eng. J. 158 (2010) 489–497.
[61] M. Islam, R.K. Patel, Evaluation of removal efficiency of fluoride from aqueous solution using quick lime, J. Hazard. Mater. 143 (2007) 303–310.
[62] Y. Hu, T. Guo, X. Ye, Q. Li, M. Guo, H. Liu, Z. Wu, Dye adsorption by resins: Effect of ionic strength on hydrophobic and electrostatic interactions, Chem. Eng. J. 228 (2013) 392–397.
[63] W. Yan, R. Vasic, A.I. Frenkel, B.E. Koel, Intraparticle reduction of arsenite (As(III)) by nanoscale zerovalent iron (nZVI) investigated with *in situ* x-ray absorption spectroscopy, Environ. Sci. Technol. 46 (2012) 7018–7026.
[64] P.H. Chang, Z. Li, J.S. Jean, W.T. Jiang, C.J. Wang, K.H. Lin, Adsorption of tetracycline on 2:1 layered non-swelling clay mineral illite, Appl. Clay Sci. 67 (2012) 158–163.